ITWCCST 2019
5th International Turkic World Conference on Chemical Sciences and Technologies
25 - 29 October, Sakarya / Turkey
2019.itwccst.org

Two-dimensional Hexagonal Boron Nitride Nanosheets Grown by Surfactant-added Exfoliation

Serra Başoğlu[1], Duygu Kuru[1], Alev Akpinar Borazan[1,*]

[1]Bilecik Seyh Edebali University, Chemical Engineering Department, Gülümbe, 11210, Bilecik

alev.akpinar@bilecik.edu.tr

Keywords: 2-D materials, boron nitride nanosheet, ionic surfactant, liquid exfoliation.

INTRODUCTION

Recent advances in understanding graphene crystals in two-dimensional (2D) order have encouraged more researchers to work in the field of nanosheets. 2D materials have a regular structure. In these materials, atoms are contained within a single layer. There are no different layers with strong or weak bonds between them [1]. The best known 2D material is graphene[2] which is the thinnest material known to date, as a single layer of a carbon honeycomb weave. Based on composition and crystal structure, many other 2D materials are known to have been predicted and synthesized in the last decade [3-6]. These materials have an ultra-thin layer structure but have different functions for different applications. Undoubtedly, because of the large number of 2D materials, their unique properties and their versatility, scientists and engineers have become interested in a wide range of research. Electronics, optoelectronics, energy storage and conversion, etc. are promising applications for 2D materials[7]. There are several methods for producing 2D materials. The best known is the micro mechanical division (MC)[2] which uses Scotch tape to separate thin layers from bulk material. Chemical vapor deposition method (CVD) is a well-known method for synthesizing nanomaterials containing zero-dimensional (OD), one-and two-dimensional (1D and 2D) materials in large quantities based on the bottom-up production principle[1]. Because of the nature of the layered nanomaterials, that is, they have strong in-plane covalent bonds between the structural components and weak van der Waals interaction between the atomic layers, it is possible to directly synthesize 2D nanosheets by exfoliation method based on 3D crystals[8].

Since boron nitride nanosheets do not effectively disperse in water, some surfactants are used for the exfoliation process. However, the concentration and lateral size of nanosheets in aqueous BNNS dispersions are quite low. To increase BNNSs concentration, ionic surfactants may be used in liquid exfoliation. At the same time, ionic surfactants provide both advantages such as effective shielding of BNNS from water and good dispersibility with water that allows it to preferably migrate to the BNNS surface and provide suspension stability[9]. Lotya et al. used SDBS ionic surfactant to produce graphene in water solution using ultrasonication technique. They successfully synthesized multilayer graphene smaller than 5 layers. They also proved that surfactant added dispersions were stable for 6 weeks[10].

Smith et al. reported the effect of 12 different ionic and non-ionic surfactant addition on production of graphene nanosheets in water suspension. For all surfactants the similar flake size obtained, and the dispersed concentration varied by a factor of 2-3 from surfactant to surfactant. It was also mentioned that ionic surfactants stabilized the sheets and played an important role to protect nanosheets from aggregation[11].

In the current paper, three kind of surfactant such as sodium dodecylsulfate (SDS) powder, sodium dodecyl benzene sulfonate (SDBS) and deoxyclic acid (DA) were used in the synthesis of boron nitride nanosheets using liquid exfoliation method. Specific ratios of surfactants and boron nitride powder were ultrasonically dispersed in water and centrifuged to form BNNSs.

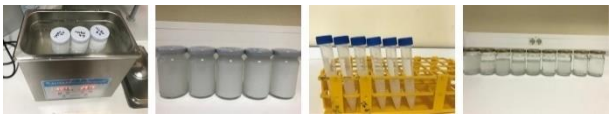

Figure 1. Ultrasonic-centrifuge technique for BNNSs production

In Figure 1 ultrasonic-centrifuge technique for BNNSs production was given. In this method, BNNSs were produced based on 5 different initial concentrations (0.2, 0.6, 0.8, 1.2, and 1.6). 3 different surfactants and boron nitride were combined to a certain extent and sonicated in an ultrasonic bath for 6 hours. It was centrifuged at 6000 rpm for 30 minutes to remove undesirable boron nitride particles. The efficiency analysis of the obtained nanosheets was determined by

UV visible region (Agilent Technologies, Cary 60 UV-Vis) spectroscopy. The morphological structure of nanosheets and surfactants was investigated by Scanning Electron Microscope (SEM, Zeiss Supra 40VP, Germany) analysis. Formation of boron nitride was proved with FT-IR (Agilent Technologies, Cary 630 FTIR) and Raman analysis. The thickness distribution of boron nitride nanosheets was determined by AFM analysis.

RESULTS AND DISCUSSION

UV-Visible Spectrophotometer was used to calculate the concentration values of boron nitride nanosheets. Table 1 shows the yield of boron nitride nanosheets after exfoliation with different surfactants.

Table 1. Concentration and yield values of boron nitride nanosheets synthesized with different surfactants

Initial concentration (mg/mL)	Surfactant	Concentration of BNNSs (mg/mL)	Yield %
0.2	SDS	0.0152	7.60
0.6	SDS	0.0121	2.01
0.8	SDS	0.0209	2.61
1.2	SDS	0.0193	1.60
1.6	SDS	0.0220	1.38
0.2	SDBS	0.0015	0.75
0.6	SDBS	0.0122	2.03
0.8	SDBS	0.0198	2.48
1.2	SDBS	0.0268	2.23
1.6	SDBS	0.0144	2.55
0.2	DA	0.0008	0.40
0.6	DA	0.0064	1.06
0.8	DA	0.0025	0.31
1.2	DA	0.0058	0.48
1.6	DA	0.0104	0.65

When the yield results of BNNSs produced using SDS surfactant were examined, concentration values varied between 0.01 and 0.02 mg/mL. These results are in parallel with SEM analysis. In the nanosheet images obtained at high concentration values, boron nitride layers were deposited on top of each other (Figure 2-d, e). At low concentrations, exfoliation and separation can be seen clearly (a, b, c). This affected the yields of the obtained nanosheets. When SDBS surfactant is used, boron nitride yields are between 0.75 and 2.5%. It was observed that the yields were lower when compared with SDS surfactant. In DA surfactant, yield results were significantly lower than both SDS and SDBS (0.3-1.06%). Figure 2,3 and 4 shows the SEM images of BNNSs with different surfactants.

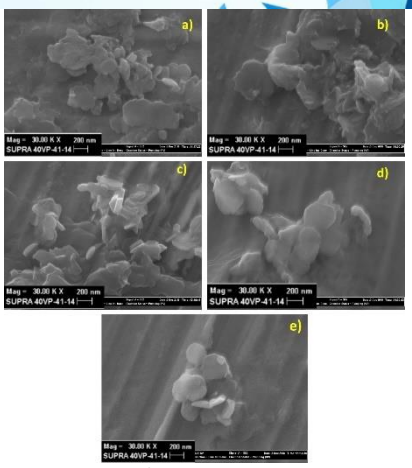

Figure 2. SEM images of boron nitride nanosheet suspensions prepared with SDS surfactant a) 02-6 b) 06-6 c) 08-6 d) 12-6 e) 16-6

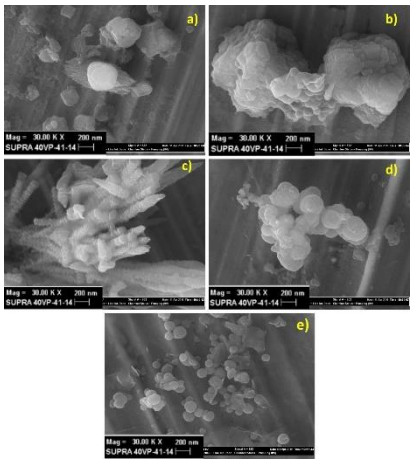

Figure 3. SEM images of boron nitride nanosheet suspensions prepared with SDBS surfactant a) 02-6 b) 06-6 c) 08-6 d) 12-6 e) 16-6

When the morphological images of BNNSs obtained using 3 different surface activators are examined, it is possible to say that SDBS is the most effective surfactant in layer-by-layer separation of boron nitride. Exfoliated layers of boron nitride were observed, especially when the initial concentration of 1.6 mg/mL was used (Figure 3-e). In Figure 3, as the initial concentration is increased, the formation of boron nitride nanosheet is more pronounced. At low concentrations, BNNSs attached to the SDBS surfactant are observed (Figure 3-c). In order to stabilize the produced 2D nanosheets, the interfacial tension between the materials and the liquid medium needs to be minimized, thus reflecting the existence of good interactions[12].

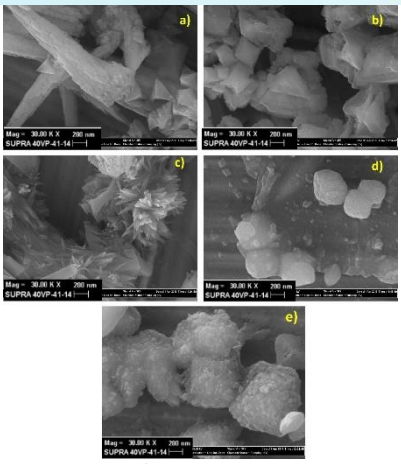

Figure 4. SEM images of boron nitride nanosheet suspensions prepared with DA surfactant a) 02-6 b) 06-6 c) 08-6 d) 12-6 e) 16-6

Figure 4 shows the typical morphological structure of the DA surfactant (Figure 4-a). It was not effective in separating boron nitride as a layer in all studied concentrations. When the efficiency results of the DA surface activator are examined, it can be said that they are in parallel with the morphological images.

Raman analysis was performed to prove the formation of BNNSs. Figure 5 shows the Raman spectra of BNNSs produced by using SDS, SDBS and DA surface activators. According to the SEM images three samples (08-SDS, 16-SDBS and 12-DA) were chosen for Raman analysis.

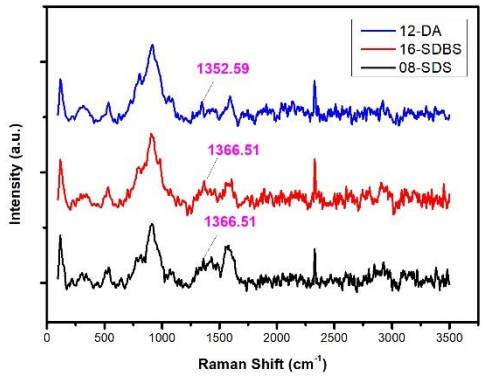

Figure 5. Raman spectra of BNNSs prepared with different surfactants

Raman spectroscopy is widely used for the characterization of lattice vibration modes of graphene-based materials. Considering shear, width and ratio between different peaks, Raman results can show the quality, layers and defect density of graphene-based materials. The typical E2g band of h-BN is about 1365 cm^{-1}; this is 1055 cm^{-1} for transverse phonons and 1305 cm^{-1} for longitudinal cubic BN [13].

This reduction in Raman density of E2g vibration can be attributed to poor interaction between layers due to exfoliation in the solvent. (002) the slight shift of the peak to the right is also associated with increased layer voids after exfoliation [14]. As the number of layers increases, the E2g band shifts to the right. From Figure 5 we can conclude that BNNSs produced with SDS and SDBS surfactants have more layers compared with the DA one as the E2g band seems at 1366.51 cm^{-1} while DA surfactant has E2g band at 1352.59 cm^{-1}.

The variation in Raman density may claim that due to the less controllable sample quantity under the irradiation of the laser spot, it may not accurately reflect the number of layers. However, the rational exfoliated BNNSs have less bulk density than h-BN bulk materials due to the greater space between the layers. In addition, increased imperfections and edge effects after exfoliation of BNNS can also be considered as the causes of E2g band change [15].

Figure 6 includes the AFM histograms of BNNSs. From Figure 6-a the thickness of nanosheets varies between 40-100 nm. The lateral dimension ranges between 1-2.5 µm.

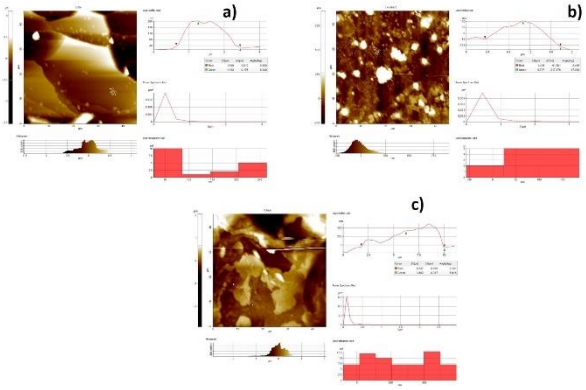

Figure 6. AFM histogram of BNNSs produced with different surfactant a) DA, b)SDBS, c)SDS

In Figure 6-b we can say that BNNSs produced with SDBS surfactant have thickness range between 0-100 nm and lateral size range is 0.4-1.8 µm. For the surfactant of SDS the thickness of BNNSs range between 0-400 nm while lateral size reaches to 10 µm. If we compare all kind of BNNSs produced with different surfactant, DA and SDBS have thinner nanosheets. BNNSs produced with SDS are thick and their lateral size is also bigger than the others.

IR spectra of boron nitride nanosheet suspensions prepared with different surfactants are similar when examined in Figure 7-9.

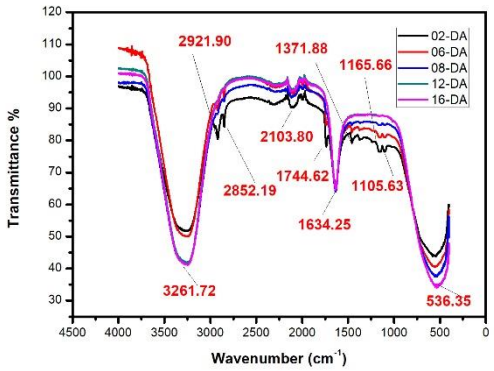

Figure 7. IR spectra of boron nitride nanosheet suspensions prepared with DA surfactant

When IR spectra are examined, it is observed that as boron nitride concentration increases, boron nitride band narrows. The stress at 3261.72 cm^{-1} wavenumbers seen in all samples belongs to the H-OH strain from the DA, SDBS and SDS structure. The peak at 2116,39 cm^{-1} belongs to strong C-C binding. Again, the sharp stress at the wavenumber of 1634.25 cm^{-1} refers to amide C = O binding[3]. It was evaluated that the stress occurring in 1371.88, 1373.88, 1377.68 belongs to the characteristic B-N-B binding mode and B-N stress in the structure of boron nitride [16]. The peak at 1165.66 cm^{-1} is the stress caused by C-C binding. At 1105.63 cm^{-1} wavenumber, the peak of the C-O-C stretch is seen. It contains the skeleton vibration bridge caused by peak S-O stretching at a wavenumber of 1220 cm^{-1}. Wide band tension of 536.35 cm^{-1} wavenumber occurred as a result of C-H asymmetric stress[3].

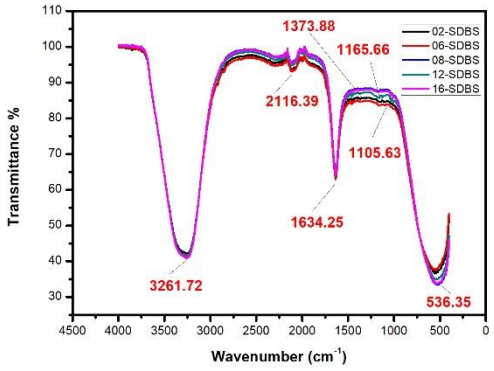

Figure 8. IR spectra of boron nitride nanosheet suspensions prepared with SDBS surfactant

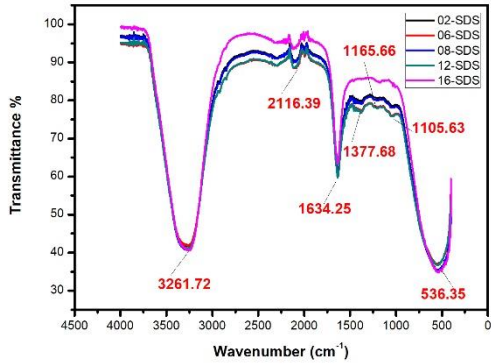

Figure 9. IR spectra of boron nitride nanosheet suspensions prepared with SDS surfactant

CONCLUSION

If the results are summarized:

- DA surfactant was not effective in separating boron nitride as a layer in all studied concentrations. According to the SEM images SDBS showed better performance as a surface activator.
- In DA surfactant, yield results were significantly lower than both SDS and SDBS (0.3-1.06%).
- The ramectrum proved that boron nitride was separated into layers. We can conclude that BNNSs produced with SDS and SDBS surfactants have more layers compared with the DA one as the E2g band seems at 1366.51 cm^{-1} while DA surfactant has E2g band at 1352.59 cm^{-1}.
- AFM histogram shows us DA and SDBS have thinner nanosheets. BNNSs produced with SDS are thick and their lateral size is also bigger than the others.

ACKNOWLEDGEMENTS

We would like to thank Bilecik Şeyh Edebali University Scientific Research Projects Unit, who supported our work with the project of 2018-01.BŞEÜ.03-06.

REFERENCES

[1] Tan, C.; Cao, X.; Wu, X.; He, Q.; Yang, J.; Zhang, X.; Chen, J.; Zhao, W.; Han, S.; Nam, G.; Sindoro, M.; Zhang, H. Chem. Rev. **2017,** 117, 6225-6331.
[2] Novoselov, K.S.; Geim, A.K.; Morozov, S.V.; Jiang, D.; Zhang, Y.; Dubonos, S.V.; Grigorieva, I.V.; Firsov, A.A. Science. **2004,** 306, 666-669.
[3] Nicolosi, V.; Chhowalla, M.; Kanatzidis, M.G.; Strano, M.S.; Coleman, J.N. Science. **2013,** 340, 1226419-18.
[4] Ma, B.R.; Sasaki, T. Adv. Mater. **2010,** 22, 5082-5104.
[5] Wang, Q.H., Kalantar-Zadeh, K.; Kis, A.; Coleman, J.N.; Strano, M.S. Nat. Nanotechnol. **2012,** 7, 699-712.
[6] Geim, A.K.; Grigorieva, I.V. Nature. **2013,** 499, 419-425.

[7] Cai, X.; Jiang, Z.; Zhang, X.; Zhang, X. Nanoscale. Res. Lett. **2018,** 13, 241.
[8] Wang, Z.; Tang, Z.; Xue, Q.; Huang, Y.; Huang, Y.; Zhu, M.; Pei, Z.; Li, H.; Jiang, H.; Fu, C.; Zhi, C. Chem. Rec. **2016,** 16, 1204- 1215.
[9] Habib, T.; Devarajan, D.S.; Khabaz, F.; Parviz, D.; Achee, T.; Khare, R.; Green, M.J. Langmuir. **2016,** 32, 1-23.
[10] Lotya, M.; Hernandez, Y.; King, P.J.; Smith, R.J.; Nicolosi, V.; Karlsson, L.S.; et al. J. Am. Chem. Soc. **2009,** 131,3611-20.
[11] Smith, R.J.; King, P.J.; Lotya, M.; Wirtz, C.; Khan, U.; De, S.; et al. Adv. Mater. **2011,** 23, 3944-8.
[12] Backes, C.; Smith, R.J.; McEvoy, N.; Berner, N.C.; McCloskey, D.; Nerl, H.C.; et al. Nat Commun. **2014,** 5,4576.
[13] Lin, Y.; Connell, J.W. Nanoscale. **2012,** 4, 6908-6939.
[14] Lin, Y.; Bunker, C.E.; Shiral Fernando, K.A.; Connell, J.W. Acs. Appl. Mater. Inter. **2012,** 4, 1110-1117.
[15] Song, L.; Ci, L.; Lu, H.; Sorokin, P.B.; Jin, C.; Ni, J.; Kvashnin, A.G.; Kvashnin, D.G.; Lou, J.; Yakobson, B.I.; Ajayan, P.M. Nano. Lett. **2010,** 10, 3209.
[16] Hou, J.; Li, G.; Yang, N.; Qin, L.; Grami, M.E.; Zhang, Q.; Wang, N.; Qu, X. RSC. Adv. **2014,** 4, 44282-44290.

ITWCCST 2019
5th International Turkic World Conference on Chemical Sciences and Technologies
25 - 29 October, Sakarya / Turkey
2019.itwccst.org

Investigation of Valproic Acid-Sensitive Biosensor Used in the Treatment of Epilepsy

Ömer Işıldak[1], Oğuz Özbek[1], Esra Özkan[2]

[1]*Tokat Gaziosmanpaşa University,Faculty of Science and Arts, Department of Chemistry, 60250 Tokat*

[2]*Tokat State Hospital, Department of Neurology,60100 Tokat*

omer.isildak@gop.edu.tr

Keywords: epilepsy, anti-epileptic, valproic acid, biosensor

INTRODUCTION

Biosensors are analytical devices that convert a biological response into an electrical signal. biosensors must be highly specific, and independent of pH, temperature and other physical parameters. In addition should be reusable. [1]. Biosensor technology is based on a specific biological recognition element (enzyme, microorganism etc) in combination with a transducer for signal processing. Biosensors have been play a significant role in medicine, agriculture, food safety, environmental and industrial monitoring [2-5].

Epilepsy is the one of the most common neurological disorder and affects people of all ages. Epilepsy is characterized by unpredictable seizures and can cause different health problems. Epileptic seizures are caused by disturbances in the electrical activity of the brain. Epilepsy is a long-term illness and its medicines are the mainstay of epilepsy treatment and sometimes the use of lifetime anti-epileptic is required. Therefore, the side effects of short and long-term treatment should be taken into consideration as well as efficacy in the treatment chosen and follow-up during use is important. Valproic acid (sodium valproate) is one of the most effective and broad-spectrum anti-epileptic drugs in epilepsy treatment. Furthermore it is one of the most widely used anti epileptics worldwide and its use is increasing day by day. Valproic acid pharmacological effects involve increased gamma-aminobutyric acid reduced release and/or effects of excitatory amino acids, blockade of voltage gated sodium channels [6].

To maintain the therapeutic blood concentration, in patients who use valproic acid, valproic acid test is performed which determine the amount of drug in the bloodstream. The normal value range of valproic acid in the blood is 50 - 100 µg / ml. If the level of blood in the drug is below this range, adequate therapeutic efficacy cannot be achieved. On the contrary, if the drug concentration in bloodstream is increases, which will cause more harm than good. In higher concentration the drug results to toxic and unwanted adverse side effects. Generally, if the level of sodium valproate is within the therapeutic limits, the patient does not have seizure recurrences, mood swings, or significant side effects in the patient and indicates that the patient uses adequate amounts of valproic acid.

This work proposal is presented for the purpose of completing a number of preliminary studies to develop a biosensor in order to follow the drug level in the blood of patients using valproic acid in the treatment of epilepsy.

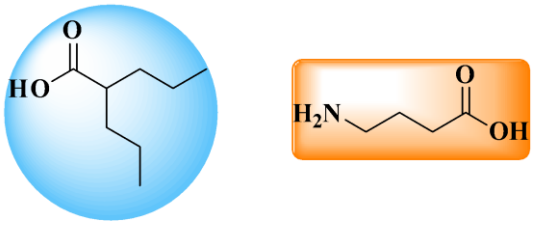

Figure 1. Structure of valproic acid and gamma-amino butyric acid (GABA)

RESULTS AND DISCUSSION

The valproic acid-selective electrode was evaluated potentiometric performance for optimize electrode composition. Valproic acid selective electrode was determined calibration curve of the over sodium valproate concentration range of 1.0 x 10^{-1} to 1.0 x 10^{-5} M.

The optimum electrode was prepared by thorough mixing of 5.5 % ionophore (gamma aminobutyric acid), 55.0 % graphite and 39.5 % epoxy in 5 mL of THF. This mixture was placed on the electrodes surface and let dry for 24 h. Prior to first use, the prepared electrodes were conditioned in a 1.0 x 10^{-2} M sodium valproate solution for 6 h. Preparation of other membranes and optimized of membrane ingredients are summarized Table 1.

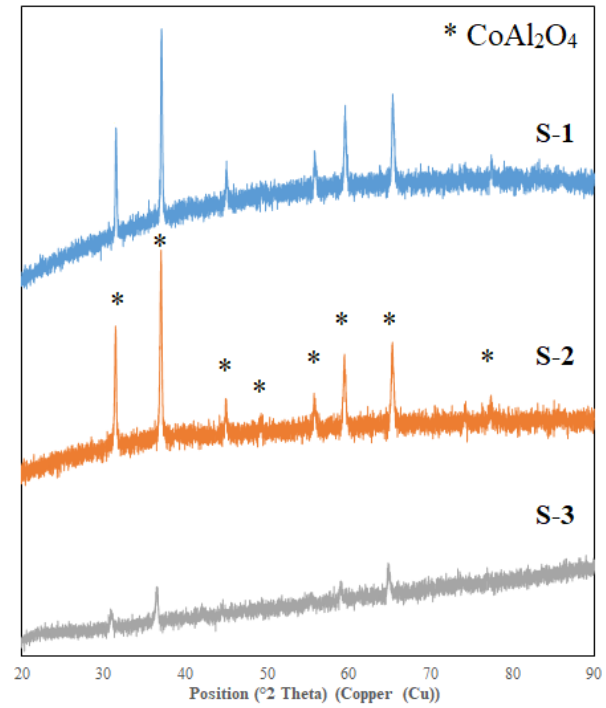

Figure 2. XRD patterns of synthesized pigments

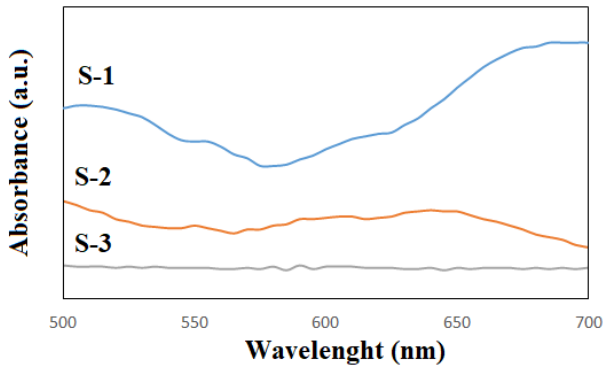

Figure 3. UV-Vis spectra of synthesized pigments

CONCLUSION

The spinel type of cobalt aluminate ($CoAl_2O_4$) is prepared with an ultrasonic assisted co-precipitation method. he effects of temperature of ultrasonic treatment on the chromatic features of synthesized pigments is experimented and characterized. For this purpose, $CoCl_2 \cdot 6H_2O$ and $AlCl_3 \cdot 6H_2O$ were reacted in liquid medium with the assistance of ultrasonic treatment at temperatures of 25, 50 and 75°C. After the obtained pink solutions were calcined at 1200°C, the intense blue particles were observed. The samples were characterized with the techniques of X-ray diffraction (XRD), UV spectroscopy and colour analysis. Experimental results indicated that ultrasonic treatment increased the colour performance of synthesized blue pigments. According to the characterization, the optimum reaction temperature is determined as 50°C.

REFERENCES

[1]Khademolhoseini, S.; Talebi, R. J. Mater. Sci.: Mater. Electron. **2016**, 27, 2938-2943.
[2]Zhang, A.; Mu, B.; Wang, X.; Wen, L.; Wang A. Front. Chem. **2018**, 6, 1-11.
[3]Rajan, K.; Roppolo, I.; Chiappone, A.; Bocchini, S.; Perrone, D.; Chiolerio, A. Nanotechnol. Sci. Appl. **2016**, 9, 1-13.
[4]Chang, Y.; Feng, T.; Wua, C.; Chen, Y.; Ke, K.; Liu, Y.; Wang, H.; Dong, S. Adv. Powder Technol. **2018**, 29, 1222–1229.
[5]Han, M.; Wang, Z.; Xu, Y.; Wu, R.; Jiao, S.; Chen, Y.; Feng, S. Mater. Chem. Phys. **2018**, 215, 251-258.
[6]Aguilar-Elguézabal, A.; Román-Aguirre, M.; De la Torre-Sáenz, L.; Pizá-Ruiz, P.; Bocanegra-Bernal, M. Ceram. Int. **2017**, 43, 15254-15257.
[7]Cains, P. W.; Martin, P. D.; Price, C. J. Org. Process Res. Dev. **1998**, 2, 34−48.
[8]Dippolito, V.; Andreozzi, G. B.; Bosi, F.; Halenius, U. Am. Min. **2012**, 97, 1828–1833.
9Gao, Y.; Chang, H.; Wu, Q.; Wang, H.; Pang, Y.; Liu; F.; Zhu, H.; Yun, Y. Trans. Nonferrous Met. Soc. China. **2017**, 27, 863−867.